Chemical Physics Letters 514 (2011) 362–367

Contents lists available at SciVerse ScienceDirect

Chemical Physics Letters

journal homepage: www.elsevier.com/locate/cplett

The quantified NTO analysis for the electronic excitations of molecular many-body systems

Jian-Hao Li [a,c], Jeng-Da Chai [a,b,*], Guang-Yu Guo [a,b,d], Michitoshi Hayashi [c,*]

[a] Department of Physics, Center for Theoretical Sciences, National Taiwan University, Taipei 10617, Taiwan
[b] Center for Quantum Science and Engineering, National Taiwan University, Taipei 10617, Taiwan
[c] Center for Condensed Matter Sciences, National Taiwan University, Taipei 10617, Taiwan
[d] Graduate Institute of Applied Physics, National Chengchi University, Taipei 11605, Taiwan

ARTICLE INFO

Article history:
Received 11 July 2011
In final form 14 August 2011
Available online 26 August 2011

ABSTRACT

We show that the origin of electronic transitions of molecular many-body systems can be investigated by a quantified natural transition orbitals (QNTO) analysis and the electronic excitations of the total system can be mapped onto a standard orbitals set of a reference system. We further illustrate QNTO on molecular systems by studying the origin of electronic transitions of DNA moiety, thymine and thymidine. This QNTO analysis also allows us to assess the performance of various functionals used in time-dependent density functional response theory.

1. Introduction

Quantum mechanical description of electronic excitations of molecular many-particle systems has been an important topic to date. Time-dependent linear response DFT (TDDFT) [1–4] has been widely used to calculate the electronic excitation energies and oscillator strengths of large molecular systems. In contrast, high-level quantum chemistry approaches such as equation of motion coupled cluster singles and doubles (EOM-CCSD) [5–9] can deal with only small systems. The TDDFT results can be, however, unreliable due to the quality of exchange–correlation functionals used. While assessment of different functionals often focuses on the excitation energies and oscillator strengths [10,11], verification of the physical origin of electronic transitions should be desirable. Casida has proposed that TDDFT wavefunction can be interpreted in terms of linear combination of singly excited configurations (LCSEC) [3]. Casida's scheme suggests that a systematic analysis can be developed so that LCSEC of TDDFT and many-body theories like EOM-CCSD can be linked for each excitation. The LCSEC contains information on transition origin that directly connects to the electronic structure change which governs the physics and chemical actions, like nuclear dynamics and chemical reactions, of an electronically excited molecule.

For assigning the transition origin of an excitation from LCSEC, the most important property is its universality. In other words, each excitation can only have one unique representation of transition origin. In this regard, we find that natural transition orbital (NTO) analysis [4,12] is a good starting point because it relies on the minimum representation of the transition operator using a NTO pair consisting of an electron- and a hole-orbital for an excitation. However, we also find that in many molecular systems, an excitation cannot be described very well by single NTO pair. One of the typical and simplest examples is a well separated dimer. Therefore, we develop a quantified NTO (QNTO) analysis that allows taking into account multi-NTO pairs properly as needed. Moreover, NTO analysis uses a pictorial description of a NTO pair that can result in ambiguity especially for large molecules with no symmetry. To establish a clear interpretation of transition origin of NTO airs, we introduce a standard-orbitals set onto which the hole- and electron-orbital of a NTO pair can be mapped. This scheme can be applied for a wide range of molecular systems, such as DNA and proteins. With QNTO analysis, we demonstrate that separate dimer can be properly described by two NTO pairs. In addition, the variation of the transition origin of an excitation due to the environment change of the system can also be determined based on the coefficient change of standard-orbitals. Furthermore, we show that TDDFT together with recently developed long-range corrected (LC) hybrid functionals [10,11,13–21] (LC-TDDFT) can predict electronic transition origins of similar quality as EOM-CCSD.

2. From NTO analysis to QNTO analysis

For single-reference linear response methods for electronic excitations, e.g. configuration interaction singles (CIS) [22], time-dependent Hartree–Fock (TD-HF) [23,24], EOM-CC, and TDDFT,

* Corresponding authors.
E-mail addresses: jdchai@phys.ntu.edu.tw (J.-D. Chai), atmyh@ntu.edu.tw (M. Hayashi).

0009-2614/$ - see front matter © 2011 Elsevier B.V. All rights reserved.
doi:10.1016/j.cplett.2011.08.066

the NTO analysis [12] is known to give a concise transition picture out of the original many SECs of an (often low-lying) excitation. This is due to the fact that mathematically some SECs in a LCSEC can be combined to form the minimum representation of transition operator. For example, let us consider an electronic excitation whose LCSEC is

$$\Psi_{ex} = 0.3\Psi_i^a + 0.5\Psi_j^a + 0.8\Psi_j^b \quad (1)$$

where, for example, $\Psi_i^a = \hat{a}_a^\dagger \hat{a}_i \Psi$ and $\hat{a}_a^\dagger$ and $\hat{a}_i$ denote, respectively, the creation operator for the ath virtual orbital and the annihilation operator for the ith occupied orbital and Ψ the ground state wavefunction of a theoretical method which may be a single determinant (e.g. in DFT) or a combination of multi-determinants (e.g. in EOM-CCSD). If one follows a NTO-generating procedure – a unitary transformation to the original occupied and virtual orbitals – the best reduced LCSEC can be achieved with an additional phase confirmation of SECs. In this case, we obtain

$$\Psi_{ex} = \sqrt{0.9172}\Psi_I^A + \sqrt{0.0628}\Psi_J^B \quad (2)$$

where $\hat{a}_I = N_I(c_1\hat{a}_i + c_2\hat{a}_j), \hat{a}_J = N_J(-c_2\hat{a}_i + c_1\hat{a}_j), \hat{a}_A^\dagger = N_A(d_1\hat{a}_a^\dagger + d_2\hat{a}_b^\dagger)$ and $\hat{a}_B^\dagger = N_B(-d_2\hat{a}_a^\dagger + d_1\hat{a}_b^\dagger)$ with $c_1 = 0.1784, c_2 = 0.9840, d_1 = 0.5696, d_2 = 0.8219$, and, for instance, $N_I = 1/\sqrt{c_1^2 + c_2^2}$. In this new description, the first SEC Ψ_I^A, corresponding to the first dominant NTO pair (NTO1), now dominates and therefore the transition picture of the excitation is clear.

However, as above mentioned, there may be a case in which the NTO1 cannot be representative to an excitation, e.g. in a separate dimer. For this reason, in the first step, we generalize the NTO analysis by taking into account the 2nd dominant NTO pair (NTO2) if the NTO1 has less than 70% domination of total LCSEC. Moreover, by checking NTO unitary matrix we also establish a procedure to determine the relative phase between NTO1 and NTO2. This phase information cannot be achieved directly from solving the eigenvalues of $\mathbf{TT}^\dagger$ and $\mathbf{T}^\dagger\mathbf{T}$ with $\mathbf{T}$ being the transition density matrix in the conventional NTO analysis, because they are simply the square of SEC coefficients, which may be positive or negative. Thus, for the negative phase combination, we have

$$\Psi'_{ex} = \sqrt{0.9172}\Psi_I^A - \sqrt{0.0628}\Psi_J^B \quad (3)$$

However, after being transformed back based on the original reference, Eq. (3) becomes

$$\Psi'_{ex} = -0.1054\Psi_i^a + 0.5735\Psi_j^a + 0.2809\Psi_i^b + 0.7491\Psi_j^b \neq \Psi_{ex} \quad (4)$$

Therefore, the phase should be correctly determined.

The correct phase can be rigorously obtained by computing the root mean square deviation of SEC coefficients between the original LCSEC and the LCSEC transformed back from the NTO-LCSEC with different phase combinations of NTO1 and NTO2. For Eq. (1), the original LCSEC is exactly equal to the one obtained from Eq. (2) because NTO1 and NTO2 have comprised all NTO-LCSEC. However, the NTO-LCSEC can, in general, contain more than two terms. In this situation, the truncated NTO-LCSEC composed of only the first two dominant terms (NTO1 and NTO2), after being transformed back, will lead to a less deviated LCSEC for the correct phase case. Following this context, adding NTO3 or higher term, as needed, can readily be done as well.

As the 2nd step of generalization, we project the hole- (NTO1-H) and electron-orbital (NTO1-E) of NTO1 onto a chosen standard orbitals set to see their quantitative involvement. The same procedure will be performed for NTO2. In doing so three advantages emerge:

(1) The precise contribution of a particular orbital-type of interest in an excitation can be computed.
We consider Eq. (1) as an example whose NTO1 is Ψ_I^A, if we simply use $\{\varphi_i, \varphi_j, \varphi_a, \varphi_b\}$ as the standard-orbitals, the proportions of φ_i and φ_j in the NTO1-H are 0.1784 and 0.9840, respectively. Similarly, the proportions of φ_a and φ_b in the NTO1-E are 0.5696 and 0.8219, respectively. Having these results, say, if φ_i and φ_j originate from the hole-orbitals of $^1n\pi^*$ and $^1\pi\pi^*$ transitions, respectively, then the precise proportion of the two orbitals in the excitation of interest can be obtained. Since NTO-based LCSEC is unique, the orbital projection would not be misleading.
(2) Improving the pictorial NTO interpretation.
Although NTO analysis can largely reduce many SECs in the original LCSEC to the dominant one or two, it is only rendered as an assistant to see the qualitative transition picture by plotting NTO1-H and NTO1-E. On the other hand, projecting NTO1(2)-H(E) to standard-orbitals set would provide a rigorous explanation of transition origin.
(3) Unification of orbital-standard for comparison.
If the exact ground state wavefunction of an electronic system can be approximated by either $|\Psi_0^{KS}\rangle$ of DFT or $|\Psi_0^{CCSD}\rangle$ of CCSD, the wavefunction up to LCSEC for an electronic excitation can be obtained within the linear response theory. However, the LCSECs given by TDDFT and EOM-CCSD are based on different references, thus making a direct comparison difficult. Furthermore, ambiguity can also arise if one compares LCSECs for excitations in two systems with different environments. Therefore, importantly, projection of

Table 1
Recovery of exciton theory prediction (TD-ωB97X) for (a) $^1\pi\pi^*$ and (b) $^1n\pi^*$ excitations. 'P' denotes the phase of NTO2. In (a) as the C6–C5′ distance, defined in Figure 1, increases, the two local transitions (NTO1, NTO2) tend to have a similar domination. The phase flipping between 9.24 and 10.24 Å may be due to a conical intersection. In contrast, in (b) two local transitions remain uncoupled regardless of the C6–C5′ distance.

(a) C6–C5′ (Å)	NTO1: "P1$_v$–S1$_v$" NTO2: "P1$_u$–S1$_u$"				P	NTO1: "P1$_u$–S1$_u$" NTO2: "P1$_v$–S1$_v$"				P
	λ (nm)	f	1st (%)	2nd (%)		λ (%)	f	1st (%)	2nd (%)	
4.24	230.4	0.104	65	32	–	228.4	0.227	65	31	+
5.24	229.6	0.114	69	28	–	228.4	0.242	69	28	+
6.24	229.3	0.118	68	28	–	228.5	0.252	68	28	+
7.24	229.2	0.119	65	32	–	228.7	0.261	65	32	+
8.24	229.1	0.118	57	39	–	228.7	0.268	57	39	+
9.24	229.0	0.118	50	46	–	228.8	0.272	50	46	+
10.24	228.8	0.270	64	33	+	229.0	0.123	64	33	–

(b) C6–C5′ (Å)	NTO1: "N1$_u$–S1$_u$"			NTO1: "N1$_v$–S1$_v$"		
	λ (nm)	f	1st (%)	λ (nm)	f	1st (%)
4.24	243.9	0.0001	99	242.14	0.0002	99
7.24	242.8	0.0002	100	242.10	0.0002	100
10.24	242.5	0.0002	100	242.11	0.0002	100

NTO1(2)-H(E) of LCSEC onto a standard-orbitals would make it possible to compare two LCSECs based on different references.

3. Results and discussion

3.1. Recovery of molecular exciton theory prediction

We demonstrate that QNTO analysis correctly recovers the molecular exciton theory [25] prediction in which a molecular homo dimer system composed of well separated geometrically identical two monomers (ideal dimer) has the formation of two excited states

$$\Psi_{ex}^{\text{dimer}} = \frac{1}{\sqrt{2}}(\varphi_u^*\varphi_v \pm \varphi_u\varphi_v^*) \quad (5)$$

where φ_u^* and φ_u is the excited and unexcited wavefunctions of monomer u and φ_v^* and φ_v those of monomer v. This situation should be reflected in QNTO analysis by having NTO1 and NTO2 as each monomer's local transition with close domination. QNTO helps verify if a real dimer system can be appropriately described by the exciton model or not. Table 1 shows this trend of two $^1\pi\pi^*$ excitations and no similar trend for two $^1n\pi^*$ ones of a real homo dimer system composed of two geometrically slightly different monomers, as shown in Figure 1, in various separations. In addition, QNTO can be applied to molecular hetero dimer as well.

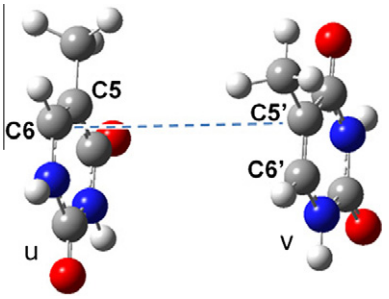

Figure 1. The Thy dimer used in Table 1 for the demonstration of molecular exciton theory recovery by QNTO analysis. In the process the distance of C6–C5′ (dash line) is modified with the two Thy base planes bearing unchanged polar angle and azimuthal angle in spherical coordinate system of z-axis along C6–C5′. In other words, the transition-dipole-transition-dipole-product of an excitation, a quantity on which the exciton theory depends, is fixed and only the distance between the two transition-dipoles is differentiated.

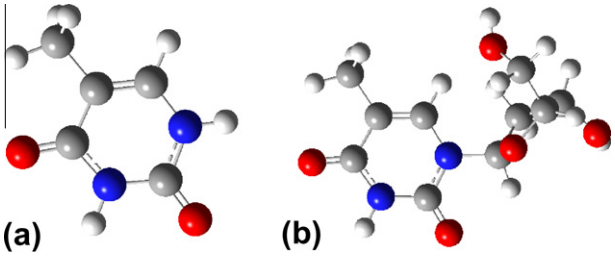

Figure 2. Molecular structures of (a) single thymine (Thy) and (b) thymidine (dT) extracted from ideal B-DNA [29]. The dT has an additional backbone structure of sugar connecting to Thy.

3.2. The LCSEC quality given by various theoretical methods

After generalizing NTO to QNTO analysis, obtaining a reliable LCSEC for an excited state is the next important concern. It depends on the use of proper approximate exchange–correlation functionals in TDDFT calculations mentioned earlier. In this regard, recently developed LC hybrid functionals, are proved to be good candidates to describe long-range transitions, and sometimes even outperform the traditional (non-LC) hybrid functionals for short-range transition as well. In a typical LC hybrid functional, 100% Hartree–Fock exchange is employed for a long-range part of the inter-electron repulsive operator $L(r)/r$, while a GGA exchange functional is employed for the complementary short-range part. Recently, Chai and Head-Gordon found that LC hybrid functionals can outperform global hybrid functionals (e.g. B3LYP [26,27]) in several important applications, such as thermochemistry, thermal kinetics, noncovalent systems, dissociation of symmetric radical cations and long-range charge-transfer excitations between two well-separated molecules [15–18]. Recent TDDFT performance tests of various LC- and non-LC hybrid functionals for predicting excitation properties of several molecular systems have been reported. Jacquemin et al. assessed the accuracy of ωB97 family for

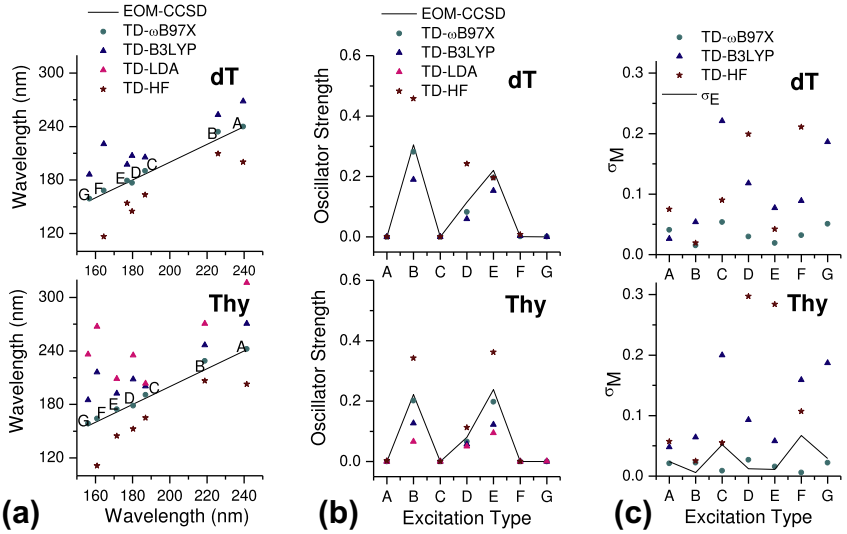

Figure 3. (a) Absorption wavelengths calculated using TD-ωB97X, TD-B3LYP, TD-LDA and TD-HF vs. absorption wavelengths from EOM-CCSD. Data of each method for the same excitation lies on the same vertical line. (b) Oscillator strength: line denotes the results from EOM-CCSD calculation. (c) σ_M of the Type-A–G calculated by the same methods except TD-LDA; σ_E is also plotted along with σ_M in the Thy result. Type-G is not predicted by TD-HF calculation for Thy whereas the excitations of dT given by TD-LDA have quite different transition origin and cannot be well-classified as Type-A–Type-G (Supporting information).

Table 2
Electronic transition origin (shown in the NTO1(2) column) of the first 7 SO-hosted singlet excitations of ideal Thy and dT given by (a) EOM-CCSD, TD-ωB97X, (b) TD-B3LYP, TD-LDA and TD-HF calculation. *N* denote the excitation order. *P* denotes the phase of NTO2 for the excitations with NTO1 domination to the LCSEC lower than 70%. % records the ratio of NTO1 to the absorption. Type denotes the excitation classification based on EOM-CCSD Thy NTO1 expressions; for EOM-CCSD the total domination of LCSEC (%) is also listed in the same column.

(a)	Ideal Thy				Ideal dT			
	N	NTO1	%	Type	*N*	NTO1	%	Type
EOM-CCSD	1	N1–S1	85	A(86)	1	N1–S1	79	A(80)
	2	P1–S1	83	B(83)	2	P1–S1	83	B(83)
	3	N1 N2–(S1) S2	86	C(88)	3	N1 N2–(S1) S2	72	C(75)
	4	P2–S1	83	D(83)	4	P2–S1	69	D(83)
	5	P1–S2	86	E(86)	5	P1–S2	75	E(84)
	6	N2–S1	83	F(85)	6	N2 (B)–S1	78	(F)(81)
	8	N1 (N2)–S2	72	G(84)	7	N1 (N2)–(S1) S2	71	(G)(75)
TD-ωB97X	1	N1–S1	100	A	1	N1–S1 (S2)	99	(A)
	2	P1–S1	97	B	2	P1–S1	97	B
	3	N1 N2–(S1) S2	99	C	3	N1 N2–(S1) S2	98	C
	4	P2–S1	99	D	4	P1–S2	96	E
	5	P1–S2	98	E	5	P2–S1	97	D
	6	N2–S1	97	F	6	N2 B (O)–S1	96	(F)
	7	N1 N2–(S1) S2	91	(G)	7	N1 N2–(S1) S2	83	(G)
(b)	Ideal Thy				Ideal dT			
	N; *P*	NTO1(2)	%	Type	*N*; *P*	NTO1(2)	%	Type
TD-B3LYP	1	N1–S1	100	A	1	N1–S1	100	A
	2	P1–S1	96	B	2	P1–S1	97	B
	3	N2–S1	93	F	3	N2 B–S1	96	(F)
	4	P2–S1	92	D	4	P2–S1	81	D
	5	N1 (N2)–S2	86	(C)	5	(N1) (N2) B–S1 (S2)	63	(C)
	6	P1–S2	89	E	+	N1 B–(S1) S2	36	
	7	(N1) N2–S2	96	(G)	6	N1 N2–S1 S2	61	(CG)
					+	N1 (N2) B–S1 S2	39	
					7	P1–S2	75	E
TD-LDA	1	N1–S1	100	A	1	N1–S1	100	A
	2	P1 (P2)–S1	97	(B)	2	(P1) B–S1	99	(B)
	3	N2–S1	100	F	3	P1 N2 (B)–S1	98	(BF)
	4	N1–S2	98	(G)	5	(P1) N2 B–S1	99	(F)
	5	(P1) P2–S1 (S2)	92	(DB)	6	N1–S2	99	(G)
	6	P1–S2	85	E	7	(P1) P2–S1 (S2)	85	(DB)
	7	N2–S2	100	(C)	9	(P1) (N2) B–S2	86	(E)
TD-HF	1	P1–S1	97	B	1	P1–S1	97	B
	2	N1 (N2)–S1 (S2) (O)	99	(A)	2	N1 (N2)–S1 (S2) (O)	98	(A)
	3	(N1) N2–S2 (O)	100	(C)	3	(N1) N2–S2 (O)	98	(C)
	4	P1 P2–S1 S2	60	(D)	4	P1–S2	71	E
	+	P1 P2–S1 S2	36		5	P2–S1 S2	80	(D)
	5	P1 P2–(S1) S2	77	(E)	7	P2–(S1) S2	88	–
	8	P2–(S1) S2	88	–	15	(P1) (N2) (B) (O)–S1 O	38	(F)
	15	N2 O–S1	71	(F)	+	P1 (N1) (N2) (O)–S1 O	32	

predicting excitation energies [10], whereas Caricato et al. focused on the simulated spectra of three molecular groups – alkenes, carbonyls and azabenzenes – in reference to EOM-CCSD results [11]. Since here we emphasize NTO1(2) transition origin of electronic excitations, several excitations of two benchmark systems-thymine (Thy) and thymidine (dT) [28] – calculated by various theoretical methods are investigated as examples.

The prepared Thy and dT (Figure 2) are extracted from ideal B-DNA structure. EOM-CCSD and TDDFT singlet excitations calculations are carried out using Gaussian09 package [30] with 6-31G(d) [31] basis set. For simplicity, solvent models are not used. EOM-CCSD, TD-ωB97X (LC hybrid functional) [15], TD-B3LYP (global hybrid functional) [26,27], TD-LDA (pure functional) [32,33] and TD-HF (exact exchange) [23,24] are demonstrated here whereas TDDFT with CAM-B3LYP [13], ωB97X-D [16], ωB97 [15], LC-ωPBE [14] (LC hybrid functionals) as well as CIS (TD-HF with Tamm–Dancoff approximation) [22] and TD-PBE1PBE (global hybrid functional) [34] are demonstrated in Figure S1 and Table SI (Supporting information).

Figure 3 and Table 2 show the results of several chosen excitations of Thy and dT. The chosen excitation, regarded as SO-hosted (standard-orbitals hosted), has its NTO1-H and NTO1-E overall more than 30% density contributions from the monomer orbitals (standard orbitals) shown in Figure 4a and b, respectively.

To determine the transition expression of a NTO1 and NTO2, we have used the following criteria: P1, for example, is involved, partial-involved and not involved in a NTO1-H if $|\langle P1|\text{NTO1-H}\rangle|^2$, density contribution of P1 to the NTO1-H, is [1,0.3], (0.3,0.1] and (0.1,0], respectively. Here $\langle P1|\text{NTO1-H}\rangle$ denotes the projection coefficient of the NTO1-H onto P1. The other transition expressions shown in Figure 4 can be determined in similar fashion. The parenthesis in the transition expression in Table 2 stands for the standard-orbital with partial-involvement. If the coefficient is negative, a standard-orbital is underlined.

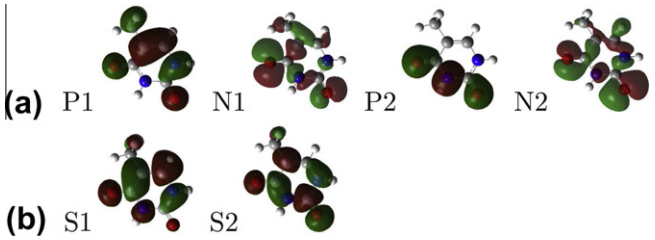

Figure 4. Standard-orbitals generated in the Thy B3LYP-DFT calculation. P1, N1, P2 and N2 correspond to the HOMO, HOMO−1, HOMO−2, and HOMO−3, respectively, and S1 and S2 are LUMO and LUMO+1. P1 and P2 (S1 and S2) are the major components of the h- (e-) orbital of $^1\pi\pi^*$-character excitations, while N1 and N2 are those of h-orbital of $^1n\pi^*$-character excitations.

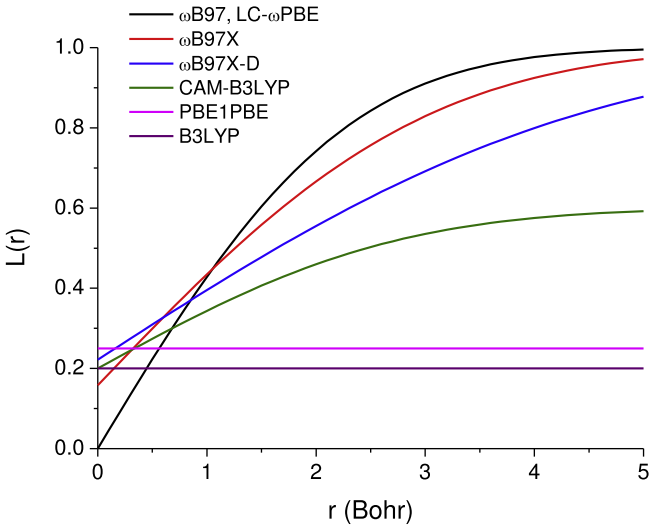

Figure 5. $L(r)$ vs. r for various functionals. $L(r)$, defined as (HF operator $* r$), is a fraction of Hartree–Fock exchange at interelectronic separation r [17].

Moreover, when dealing with dT we also introduce 'B' referring to all orbital-fraction of NTO1-H from the DNA sugar backbone attaching to Thy. The integration of standard-orbitals (plus 'B' for dT) generally accounts for more than 90% of a NTO1(2)-H(E). Otherwise, we attribute the involvement of all other Thy orbitals as 'O', which is given in the parenthesis if its contribution is (0.3, 0.1].

From Table 2, it can firstly be seen in EOM-CCSD results that the low-lying excitations indeed can be well described by LCSEC, as its total domination to whole excitation is generally higher than 0.80 (0.75 to be the lowest); secondly their LCSEC can generally be well explained by NTO1, as its domination is often close to the LCSEC one (NTO2 may arise for higher-lying excitations or the dimer systems mentioned earlier). Panels a and b in Figure 3 compare the calculated resonance wavelengths and the corresponding oscillator strengths using various theoretical methods. One can readily see that TD-ωB97X results highly agree with those of EOM-CCSD. Moreover, Table 2 shows that the TD-ωB97X can accurately reproduce the transition origin expressions EOM-CCSD predicts as well.

To confirm this more rigorously, we perform a precise statistical assessment of NTO1 of an excitation, where the root mean square deviation of the projection coefficients (σ) of NTO1-H and NTO1-E of each electronic transition is computed. σ_M is used when we map the NTO1 obtained from TDDFT with various functionals or other theoretical methods onto NTO1 of EOM-CCSD and σ_E is for comparison between EOM-CCSD results for Thy and dT. Panel c in Figure 3 shows the results of the statistical assessment, which clearly demonstrates excellent agreement between EOM-CCSD and TD-ωB97X calculations in terms of the predicted NTO1 transition origin even for the small system Thy. Other comparisons are presented in Figure S1 and Table SI. We also notice that EOM-CCSD provides generally smaller NTO1 domination than TDDFT does even for the lowest excitation of Thy. This is attributed to the limitation of adiabatic approximation of exchange–correlation kernel used in this Letter [35]. In other words, TDDFT renders LCSEC to be 100% of an excitation. Similar situation occurs for TD-HF and CIS calculations (Supporting information). Furthermore, LCSEC from LC-TDDFT agrees well with that of EOM-CCSD in that the relative percentage of different SECs is well reproduced. Therefore, the σ_M of LC-TDDFT for the low energy Type-A–Type-G absorptions is very small.

The key factor causing functionals to have the results of different quality is their HF-exchange prescription, as shown in Figure 5. Global hybrid functionals, like B3LYP and PBE1PBE, bear increased self-interaction error (SIE) for charge-transfer transition component with systematic underestimation of transition energy. Instead, LC hybrid functionals, implemented with a distance-dependent HF-exchange, can efficiently reduce SIE. In [17], it has been argued that LDA and GGAs (semilocal density functionals) are accurate only for small interelectronic separations (r). Even though how precisely the amount of HF-exchange should change with r remains unknown [21], the importance of HF-exchange generally grows with an increasing r. Compared with the results of other theoretical methods used, we find that TD-ωB97X, having the smallest average σ_M, best reproduces the NTO1 transition origin that EOM-CCSD predicts for the several low-lying excitations of Thy and dT without sacrificing other excitation properties. Hence it is a very good choice to use when studying the electronic excitations of DNA systems. For other molecular systems more tests may still be needed; for open-shell systems the use of present model also requires extra consideration where the ground state wavefunction is often no-longer dominated by a single Slater determinant.

4. Conclusion

In this Letter, we have established the basic concept of QNTO analysis and also demonstrated it by systematically studying the transition origin of the low-lying electronic excitations of two DNA moieties. We have quantitatively interpreted the transition origin of these electronic excitations by mapping them onto a standard orbitals set of a reference system. This provides the fingerprint of electronic excitations and allows us to further perform a measure of transition origin variation of particular excitations (e.g. SO-hosted ones in this Letter) due to a variation of environment (σ_E). In addition, QNTO can also be used to benchmark different theoretical methods (σ_M) in reference to highly accurate theories like EOM-CCSD. We find that TDDFT with several LC hybrid functionals (CAM-B3LYP, LC-sPBE, ωB97 family) outperform several other traditional methods in predicting transition origin of electronic excitation of these two DNA moieties, which have not yet been systematically investigated by previous theoretical assessment works.

We anticipate the following outlooks of QNTO analysis: (1) once the transition origins are determined, one can study the electronic structure changes that are important for later molecular dynamics (nuclear motions, non-radiative transitions, photo-induced chemical reactions, etc.), (2) QNTO can be used to investigate low-lying electronic excitations of a molecule with low or even no symmetry, inevitable for bio-molecules surrounded by various symmetry-breaking environments or grown with complex structures, (3) since the computational cost is moderate, LC-TDDFT combined with QNTO analysis is expected to be particularly useful in studying larger bio-molecular systems, and (4) since QNTO concept is not specific to bio-molecules, other categories of molecular systems may be studied in a similar fashion.

Acknowledgments

We thank National Science Council and NCTS of Taiwan for supports. MH would like to thank NSC for the financial support (NSC 100-2113-M-002-005).

Appendix A. Supplementary data

Supplementary data for the other details of QNTO analysis, the results of other theoretical methods, and the projection coefficients of QNTOs analysis can be found, in the online version, at doi:10.1016/j.cplett.2011.08.066.

References

[1] E. Runge, E.K.U. Gross, Phys. Rev. Lett. 52 (1984) 997.
[2] M.A.L. Marques, C.A. Ullrich, F. Nogueira, A. Rubio, K. Burke, E.K.U. Gross (Eds.), Time-Dependent Density Functional Theory, Springer-Verlag, 2006.
[3] M.E. Casida, in: D.P. Chong (Ed.), Recent Advances in Density Functional Methods, vol. 1, World Scientific, Singapore, 1995.
[4] A. Dreuw, M. Head-Gordon, Chem. Rev. 105 (2005) 4009.
[5] R.J. Bartlett, M. Musial, Rev. Mod. Phys. 79 (2007) 291.
[6] H. Koch, P. Jørgensen, J. Chem. Phys. 93 (1990) 3333.
[7] J.F. Stanton, R.J. Bartlett, J. Chem. Phys. 98 (1993) 7029.
[8] H. Koch, R. Kobayashi, A. Sánchez de Merás, P. Jørgensen, J. Chem. Phys. 100 (1994) 4393.
[9] M. Kállay, J. Gauss, J. Chem. Phys. 121 (2004) 9257.
[10] D. Jacquemin, E.A. Perpète, I. Ciofini, C. Adamo, Theor. Chem. Acc. 128 (2011) 127.
[11] M. Caricato, G.W. Trucks, M.J. Frisch, K.B. Wiberg, J. Chem. Theory Comput. 7 (2011) 456.
[12] R.L. Martin, J. Chem. Phys. 118 (2003) 4775.
[13] T. Yanai, D. Tew, N. Handy, Chem. Phys. Lett. 393 (2004) 51.
[14] O.A. Vydrov, J. Heyd, A.V. Krukau, G.E. Scuseria, J. Chem. Phys. 125 (2006) 074106.
[15] J.-D. Chai, M. Head-Gordon, J. Chem. Phys. 128 (2008) 084106.
[16] J.-D. Chai, M. Head-Gordon, Phys. Chem. Chem. Phys. 10 (2008) 6615.
[17] J.-D. Chai, M. Head-Gordon, Chem. Phys. Lett. 467 (2008) 176.
[18] J.-D. Chai, M. Head-Gordon, J. Chem. Phys. 131 (2009) 174105.
[19] A. Savin, in: J.M. Seminario (Ed.), Recent Developments and Applications of Modern Density Functional Theory, Elsevier, Amsterdam, 1996, pp. 327–357.
[20] H. Iikura, T. Tsuneda, T. Yanai, K. Hirao, J. Chem. Phys. 115 (2001) 3540.
[21] J.A. Parkhill, J.-D. Chai, A.D. Dutoi, M. Head-Gordon, Chem. Phys. Lett. 478 (2009) 283.
[22] J.B. Foresman, M. Head-Gordon, J.A. Pople, M.J. Frisch, J. Phys. Chem. 96 (1992) 135.
[23] T.D. Bouman, A.E. Hansen, Chem. Phys. Lett. 117 (1985) 461.
[24] V.J. Galasso, Mol. Struct. (THEOCHEM) 168 (1988) 161.
[25] M. Kasha, Radiat. Res. 20 (1963) 55.
[26] A.D. Becke, J. Chem. Phys. 98 (1993) 5648.
[27] C. Lee, W. Yang, R.G. Parr, Phys. Rev. B 37 (1988) 785.
[28] C.E. Crespo-Hernández, B. Cohen, P.M. Hare, B. Kohler, Chem. Rev. 104 (2004) 1977.
[29] A.G. Leslie, S. Arnott, R. Chandrasekaran, R.L. Ratliff, J. Mol. Biol. 143 (1) (1980) 49.
[30] M.J. Frisch et al., Gaussian09, Revision A.1, Gaussian, Inc., Wallingford, CT, 2009.
[31] R. Ditchfield, W.J. Hehre, J.A. Pople, J. Chem. Phys. 54 (1971) 724.
[32] J.C. Slater, in: The Self-Consistent Field for Molecular and Solids, Quantum Theory of Molecular and Solids, vol. 4, McGraw-Hill, New York, 1974.
[33] S.H. Vosko, L. Wilk, M. Nusair, Can. J. Phys. 58 (1980) 1200.
[34] C. Adamo, V. Barone, J. Chem. Phys. 110 (1999) 6158.
[35] N.T. Maitra, F. Zhang, R.J. Cave, K.J. Burke, J. Chem. Phys. 120 (2004) 5932.